

University of Groningen

Chiral separation by enantioselective liquid-liquid extraction

Verkuijl, Bastiaan Jeroen Victor

IMPORTANT NOTE: You are advised to consult the publisher's version (publisher's PDF) if you wish to cite from it. Please check the document version below.

Document Version

Publisher's PDF, also known as Version of record

Publication date:

2009

[Link to publication in University of Groningen/UMCG research database](#)

Citation for published version (APA):

Verkuijl, B. J. V. (2009). *Chiral separation by enantioselective liquid-liquid extraction: from novel systems to continuous multistage processes*. s.n.

Copyright

Other than for strictly personal use, it is not permitted to download or to forward/distribute the text or part of it without the consent of the author(s) and/or copyright holder(s), unless the work is under an open content license (like Creative Commons).

The publication may also be distributed here under the terms of Article 25fa of the Dutch Copyright Act, indicated by the "Taverne" license. More information can be found on the University of Groningen website: <https://www.rug.nl/library/open-access/self-archiving-pure/taverne-amendment>.

Take-down policy

If you believe that this document breaches copyright please contact us providing details, and we will remove access to the work immediately and investigate your claim.

Downloaded from the University of Groningen/UMCG research database (Pure): <http://www.rug.nl/research/portal>. For technical reasons the number of authors shown on this cover page is limited to 10 maximum.



Chapter 2

**Chiral Separation of Primary Amines
with Phosphoric Acids**

Chapter 2

Abstract

In this chapter it is shown that 3,3'-diaryl-BINOL phosphoric acids are effective enantioselective extractants in chiral separation methods based on reactive liquid-liquid extraction. These new extractants are capable of separating racemic benzylic primary amine substrates. The effect of the nature of the substituents at the 3,3'-positions of the host was examined as well as the structure of the substrate, together with important parameters such as the organic solvent, the pH of the aqueous phase and the host stoichiometry. Titration of the substrate with the host was monitored by FTIR, NMR, UV-Vis and CD spectroscopy, which provides insight into the structure of the host-guest complex involved in these extractions.

2.1 Introduction

In the field of enantioselective liquid-liquid extraction (ELLE), a considerable effort has been devoted to the separation of functionalized primary amines, in particular protected α -amino acids and amino-alcohols, due to their importance for the fine chemical and pharmaceutical industries. The seminal work of Cram *et al.* on the extraction of α -amino acid esters using crown ethers featuring a chiral BINOL backbone,^{1,2} resolution of amino-alcohols with good selectivities using azophenolic crown-ethers^{3,4} and the recent work of Kim *et al.* on the separation of amino alcohols using stereoselective imine hydrolysis⁵ demonstrate the potential of ELLE.

A pressing issue with the use of ELLE as a viable separation technique is the development of improved chiral host compounds.⁶ Compounds with a phosphoric acid functionality have proven to be suitable hosts in reactive liquid-liquid extraction. Bis(2-ethylhexyl) hydrogen phosphate (D2EHPA) showed to be an effective host for the reactive liquid-liquid extraction of metal cations⁷ and α -amino acids.⁸ In combination with a tartaric acid derivative, Luo *et al.* have reported ELLE combined with classic resolution by crystallization of tryptophan with an operational selectivity up to 5.3.⁹

However, one of the main challenges within the field of ELLE is the selective extraction of non-functionalized primary amines. Until now, additional groups in the host and in the substrate were needed for enantioselective host-guest recognition. Hence, intermediates such as α -methylbenzylamine (Mba) and phenylpropylamine (Ppa) which only contain a primary amine at a benzylic position, are not easily separated. An enantiomerically pure host bearing a phosphoric acid functionality would be a good candidate for the separation of racemic primary amines.

In this chapter, it is demonstrated that the newly developed hosts, 3,3'-disubstituted binaphthyl-phosphoric-acids (BNPA), are capable of

Chapter 2

extracting Ppa with the highest operational selectivity reported to date. The hosts also allow the extraction of a range of amino alcohols with significant selectivity.

The design of the host has to meet a number of conditions in order to be generally applicable to a particular substrate class. Ideally, an ELLE system consists of an organic phase and a buffered aqueous phase. Hence, the host should be confined to one phase of the system and the physical partitioning of the host should be as low as possible. In the majority of systems reported to date, a lipophilic host confined to the organic phase has been employed. Furthermore, the substrate must have a physical partitioning (which is defined as the distribution in absence of the host) as low as possible, to avoid non-enantioselective diffusion into the organic phase and, by default, the substrate must be susceptible to reactive extraction. To make the system useful for fractional extraction, back-extraction of the substrate must be possible also, which may entail adjusting the pH of the aqueous layer to achieve full back extraction.

In the present study a 3,3'-disubstituted BINOL was chosen as the chiral motif in the host. Its axial chirality makes enantioselective recognition possible.¹⁰ A phosphoric acid functionality is used to set the axial structure and to increase the Brønsted acidity of the host. Additionally, it acts as a Lewis base and may generate further hydrogen bonding interactions.¹⁰

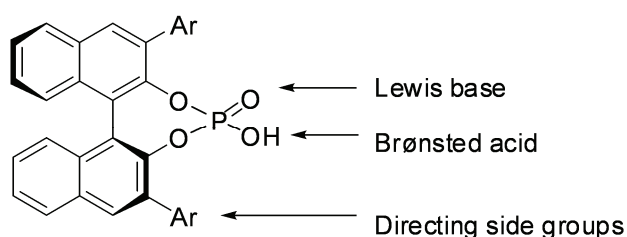


Figure 2.1 Host design

The axial chirality of the host provides for enantiomeric recognition at the phosphoric acid site. The recognition is expected to be enhanced by placing

substituents at the 3,3'-positions of the BINOL backbone to generate a "chiral cleft" (Figure 2.1).¹¹ Electron-deficient phenyl rings e.g. 3,5-bis-trifluoromethyl-phenyl moieties (PA1), may enable enhanced π - π -stacking interactions with the electron-rich benzylic amines (Figure 2.2). The non-substituted BNPA (PA2) is used as a reference compound whereas PA3 is employed to examine the role of the trifluoromethyl groups present in PA1. The biphenyl functionality in PA4 is employed to introduce additional steric bias.

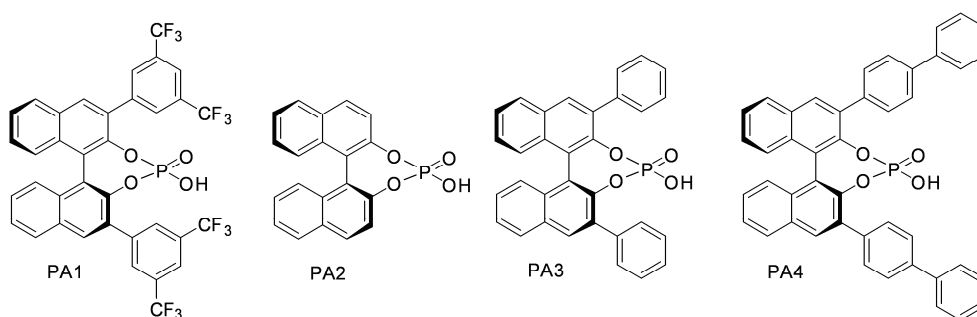


Figure 2.2 BINOL based phosphoric acids (PA1-PA4)

2.2 Results and discussion

2.2.1 Single extraction experiments

Substrate scope

PA1 was employed in the enantioselective extraction of a number of amines and amino-alcohols (Figure 2.3) to test the versatility of the system.

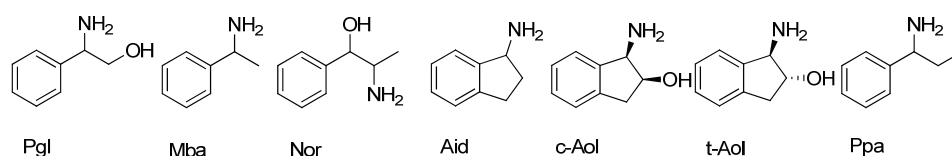


Figure 2.3 Substrate structures. Pgl = Phenylglycinol, Mba = α -Methylbenzylamine, Nor = Norephedrine, Aid = Aminoindane, c-Aol = *cis*-1-Amino-2-indanol, t-Aol = *trans*-1-Amino-2-indanol, Ppa = Phenylpropylamine.

The physical partition is 0.0 for all used substrates and the distribution of all substrates is in the range of 1.0 at pH = 5.0. With Mba, a distribution of 1.2 and an operational selectivity of 1.6 was obtained. A distribution exceeding 1.0 suggests the binding of a second guest molecule to the host.^{12,13} The presence of an alcohol group in the substrate (Pgl) leads to an increase in selectivity to 1.9. Interchanging the alcohol and amine positions in the amino alcohol structure in the substrate (Nor) results in complete loss in selectivity. This indicates that the amine functionality needs to be at the benzylic position to obtain selectivity. The results with Ppa (entry 4) show that the addition of an extra methyl group has a large effect and leads to an almost complete loss of selectivity. Hence the ability of PA1 to extract a substrate in an enantioselective manner is highly dependent on the substrate's structure.

Chiral Separation of Primary Amines with Phosphoric Acids

Table 2.1 Substrate scope.

Entry	Substrate	$P(\text{org/aq})$	$D(\text{org/aq})^{[a]}$	$\alpha_{\text{op}}^{[b]}$
1	Mba	0.0	1.2	1.6
2	Pgl	0.0	1.2	1.9
3	Nor	0.0	1.1	1.0
4	Ppa	0.0	1.2	1.1
5	Aid	0.0	1.2	1.2
6	t-Aol	0.0	0.9	1.4
7	c-Aol	0.0	0.7	1.1

Conditions: host = PA1; organic phase = CCl_4 ; pH(aqueous phase) = 5.0. [a] The distribution $D(\text{org/aq})$ of the substrate (AA) over the two phases is defined as the ratio of the concentration of the substrate over the two phases ($D = [\text{AA}]_{\text{org}}/[\text{AA}]_{\text{aq}}$) [b] The operational selectivity (α_{op}) is defined as the ratio of distribution of enantiomers ($\alpha_{\text{op}} = D_{\text{D-AA}}/D_{\text{L-AA}}$).

When the relative position of the amine and the aromatic ring are fixed, as in Aid, a partial loss in selectivity is observed. Comparing Pgl with t-Aol, the amine and alcohol of the t-Aol appear not to be in an optimal orientation, and this is more so in the case of c-Aol. The relative rotational freedom of the amine and the alcohol present in the Pgl appears to be essential for selectivity.

Influence of the host structure

The structure of the host has a critical impact on the operational selectivities observed. With the exception of PA1, all hosts gave a suspension when CCl_4 was used as the organic phase. Hence chloroform was chosen to compare the relative selectivity of the hosts.

Chapter 2

Table 2.2 The influence of the host structure on the ELLE of amine substrates.

Entry	Host	Substrate	$D(org/aq)$	α_{op} ^[a]
1	PA1	Pgl	1.0	1.7 (<i>S</i>)
2	PA2 ^[a]	Pgl	0.2	-
3	PA3	Pgl	0.8	1.2 (<i>S</i>)
4	PA4	Pgl	0.7	-
5	PA1	Mba	1.2	1.4 (<i>S</i>)
6	PA2 ^[a]	Mba	0.0	-
7	PA3	Mba	1.0	1.3 (<i>R</i>)
8	PA4	Mba	1.1	1.4 (<i>S</i>)
9	PA1	Ppa	1.2	-
10	PA2 ^[a]	Ppa	3.5	1.2 (<i>R</i>)
11	PA3	Ppa	1.1	1.2 (<i>R</i>)
12	PA4	Ppa	0.9	1.7 (<i>S</i>)

Conditions: organic phase = CHCl₃; pH(aqueous phase)=5.0 [a] c(PA2) 2.0 mM. [a] The preferred extracted enantiomer is added in brackets.

The role played by the 3,3'-substituents in the enantiospecific interaction between PA1 and Pgl is evident from entries 1-4 of Table 2.2. A high selectivity is observed for PA1. The lack of the 3,3'-substituents (entry 2) leads to a complete loss of selectivity and also a large decrease in the extraction efficiency. Entry 3 demonstrates the necessity of the trifluoromethyl groups in achieving selectivity, where the phenyl-substituted host provides an α_{op} of only 1.2.

With Mba and Ppa, a remarkable reversal in α_{op} is observed. In both cases, PA3 shows a preference for the (*S*) enantiomer (entries 7 and 11) with moderate selectivity. This preference is reversed to the (*R*) enantiomer when a 4,4'-biphenyl group is present in the host (entries 8 and 12) and is PA4 also able to separate Ppa with high selectivity (Entry 12).

Influence of the solvent

The organic solvent can have a profound influence both on the distribution and the operational selectivity in enantioselective host-guest complexations, due to the effect on noncovalent interactions caused by the difference in solvation and the influence that the solvent can have on the conformation of the complex.¹⁴

Table 2.3 Solvent dependency on $P(\text{org/aq})$, $D(\text{org/aq})$ and α_{op} with Mba, Pgl and Ppa.

Entry	substrate	solvent	$P(\text{org/aq})$	$D(\text{org/aq})$	α_{op}
1	Mba	1-octanol	0.0	0.9	1.0
2	Mba	nitrobenzene	0.0	1.2	1.1
3	Mba	1,2-dichloroethane	0.0	1.0	1.4
4	Mba	dichloromethane	0.0	0.9	1.2
5	Mba	chloroform	0.0	1.0	1.4
6	Mba	chlorobenzene	0.0	1.2	1.3
7	Mba	toluene	0.0	1.1	1.3
8	Mba	carbon tetrachloride	0.0	1.2	1.6
9	Pgl	1-octanol	0.0	0.7	1.6
10	Pgl	nitrobenzene	0.0	1.0	1.7
11	Pgl	1,2-dichloroethane	0.0	0.9	1.6
12	Pgl	dichloromethane	0.0	0.8	1.6
13	Pgl	chloroform	0.0	0.8	1.7
14	Pgl	chlorobenzene	0.0	1.1	1.7
15	Pgl	toluene	0.0	1.0	1.6
16	Pgl	carbon tetrachloride	0.0	1.0	1.9
17	Ppa	1-octanol	0.0	0.9	1.0
18	Ppa	nitrobenzene	0.0	1.2	1.1
19	Ppa	1,2-dichloroethane	0.0	0.9	1.0
20	Ppa	dichloromethane	0.0	0.9	1.1
21	Ppa	chloroform	0.0	1.0	1.0
22	Ppa	chlorobenzene	0.0	1.2	1.0
23	Ppa	toluene	1.3	1.1	1.0
24	Ppa	carbon tetrachloride	0.0	1.2	1.1

Conditions: host = PA1; pH(aqueous phase) = 5.0; T = 6 °C

Chapter 2

The physical partition of the substrates Pgl, Mba and Ppa is 0.0 throughout the library of organic solvents presented here, with the exception of Ppa in toluene as seen in entry 23 of Table 2.3. The distributions fall within the range of 0.7-1.2. The ELLE of Mba shows solvent dependence of the selectivity. In polar solvents such as 1-octanol or nitrobenzene (entry 1 and 2), selectivity is not observed. In the case of the most apolar solvent (CCl₄, entry 8) a maximum selectivity of 1.6 is obtained. Interestingly, the extraction of Pgl does not show the same solvent dependence. In this case the selectivity is essentially constant throughout the range of solvents examined, with the exception of CCl₄ which provides a higher selectivity (1.9). The ELLE of Ppa shows, as with the other substrates, a constant distribution throughout the solvent range, with the selectivity being independent of the solvent.

The selectivity in the extraction of Mba is proposed to be influenced by the nature of the ion pair formed by PA1 and Mba. The lower the polarity of the solvent, the closer the contact in the ion pair¹⁵ and hence the higher the selectivity.^{6,16} In the case of Pgl, the alcohol functionality of the substrate is proposed to have a dominating effect. Another factor that might play a role is the presence of water in the system. Water is known to affect the enantioselectivity in organocatalysed reactions with chiral phosphoric acid type catalysts.¹⁷ Also, *ab initio* studies of complexes formed by triethylamine, formic acid and water showed the preference for formation of a neutral monohydrated complex over a monohydrated ion pair.¹⁸

Influence of the pH of the aqueous phase

The pH of the aqueous phase was varied to study its influence on the distribution and operational selectivity of the extraction. In the pH-range of 3.0-8.0 the extraction was examined using the optimal organic solvent CCl₄ (*vide supra*). An aqueous suspension is obtained at pH values above 8.0, due to back-extraction of host into the aqueous phase.

Chiral Separation of Primary Amines with Phosphoric Acids

Table 2.4 pH dependency.

Entry	pH	P (org/aq)	D(org/aq)	α_{op}
1	3.0	0.0	0.3	2.1
2	4.0	0.0	1.0	2.0
3	5.0	0.0	1.0	1.9
4	6.0	0.0	1.1	2.0
5	7.0	0.0	1.1	1.9
6	8.0	0.0	1.2	1.9

Conditions: host = PA1; substrate = Pgl; organic solvent = CCl₄

At pH values below 4.0, the distribution is reduced due to the preferential ammonium state of the substrate. For example, the distribution at pH = 3.0 (entry 1) in the case of carbon tetrachloride is 0.3 (Table 2.4); a value that increases to 1.0 at pH = 4.0 (entry 2). At pH 4.0 and lower the substrate is largely confined to the aqueous phase as its ammonium cation. The pK_b of phenylglycinol is 5.5. Altogether the phenylglycinol is >99% in its ammonium cation state at pH = 4.0 and at this pH value, a D(org/aq) of 1.0 is still achieved. This is presumably due to a high association constant between the host and the substrate, because of the acidity of the phosphoric acid group of PA1 (the pK_a of (EtO)₂P(O)OH is 1.3¹⁹). The operational selectivity in the pH range 3.0 to 8.0 is between 1.9 and 2.1 with CCl₄ as a solvent. Within this pH range, no clear correlation between the operational selectivity and the pH is observed.

Influence of the host/guest stoichiometry

In Table 2.5 the results of a study on the relationship between the stoichiometry of the host and the substrate are shown. The substrate is held at a constant concentration (2.0 mM), whereas the host concentration was varied over the range 0.4 to 2.0 mM. The pH of the aqueous phase was maintained at 3.0, to keep the distribution at values between 0.1 and 0.6. The distribution and the ee in the aqueous layer increase with the increase of the host stoichiometry. The ee (org) shows a reversed relationship, i.e. the ee in the organic layer decreases as the host/guest stoichiometry increases.

Chapter 2

The operational selectivity is independent of the host/substrate stoichiometry.

Table 2.5 Dependence of $D(\text{org/aq})$, α_{op} and ee on host/substrate stoichiometry.

Entry	$c(\text{host})(\text{mM})$	$D(\text{org/aq})$	α_{op}	ee (aq)	ee (org)
1	0.4	0.1	2.3	4	36
2	0.6	0.2	2.2	5	33
3	0.8	0.2	2.2	7	32
4	1.0	0.3	2.3	9	32
5	1.2	0.4	2.2	10	29
6	1.4	0.4	2.2	11	28
7	1.6	0.5	2.2	13	26
8	2.0	0.6	2.2	15	23

Conditions: host = PA1; substrate = Pgl; organic phase = CCl_4 ; pH(aq phase) = 3.0.

Influence of the temperature and the concentration

The extraction of Pgl with PA1 in CCl_4 showed no significant change of distribution and selectivity from $T = 6\text{ }^\circ\text{C}$ to room temperature. The concentration of the substrate can be increased from 2.0 to 100.0 mM, with the host concentration being increased accordingly. The ee is constant over this range. For applications, this is an important property, since concentrations in the 0.1 M regime are necessary to achieve a satisfying throughput in a contact separator cascade.²⁰

2.2.2 Spectroscopy

Because of the high α_{op} in extraction, the chiral separation of Pgl using PA1 was chosen as a benchmark system in spectroscopic studies with the aim of gaining further insight into the mechanism of host/substrate complexation.

¹H-NMR Spectroscopy

NMR spectroscopy can be a powerful tool in the determination of the stoichiometry and equilibria involved in host-guest complexation.²¹ If the

phosphoric acid in the host is susceptible to hydrogen bonding or ion pairing with an appropriate guest, a change in the ^1H -NMR spectra is anticipated.

Titration curves for both of the enantiomers of Pgl in CDCl_3 with the host PA1 are shown in Figure 2.4. The concentration of PA1 is held constant at $c = 1.0 \text{ mM}$, i.e. the ordinate represents both the concentration of Pgl (mM) and the $[\text{Pgl}]/[\text{PA1}]$ ratio. The change in chemical shift of the ^1H -NMR absorption of the proton of the phosphoric acid group PA1 is plotted against the $[\text{Pgl}] : [\text{PA1}]$ ratio.

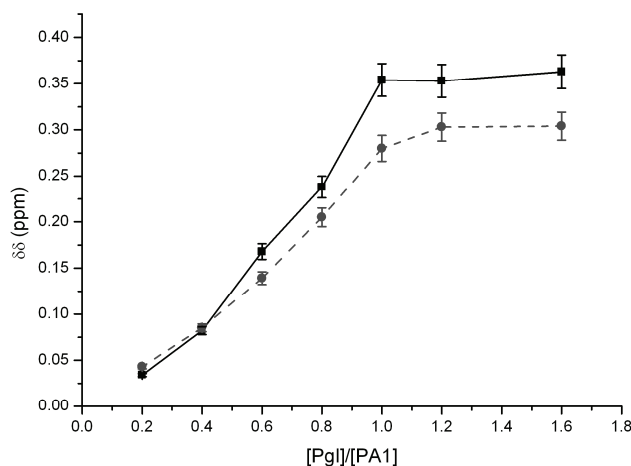


Figure 2.4 Change in chemical shift of the phosphoric acid proton of PA1 upon titration of (*R*)-Pgl (solid) and (*S*)-Pgl (dashed). Error bars represent 5% standard deviation.

This absorption shifts towards lower field upon titration with Pgl. This downfield shift is consistent with the interaction of the acidic proton with an amine group.²² The maximum is reached at a ratio of $[\text{Pgl}]/[\text{PA1}] = 1.0$, supporting the formation of a 1:1 complex of the host with the substrate. The maximum in the change in chemical shift is at 0.36 ppm for (*R*)-Pgl and 0.30 ppm for (*S*)-Pgl, reflecting the difference between the chemical shifts of the diastereomeric complexes.

FTIR Spectroscopy

Fourier Transform Infrared Spectroscopy (FTIR) spectroscopy titration experiments were performed in a similar manner to the NMR-titration experiments described above. The concentration of PA1 was held constant at $c = 1.0$ mM and the concentration of Pgl was increased incrementally from 0.2 mM to 1.4 mM. The FTIR spectra of PA1 with (*R*)-PGL are depicted in Figure 2.5. Pgl shows no absorption bands in the region given here. PA1 shows the absorption bands as described in the literature (1474, 1462, 1427, 1377, 1358, 1335, 1281, 1236, 1182, 1140, 1036, 989, 897, 845 cm^{-1})²³

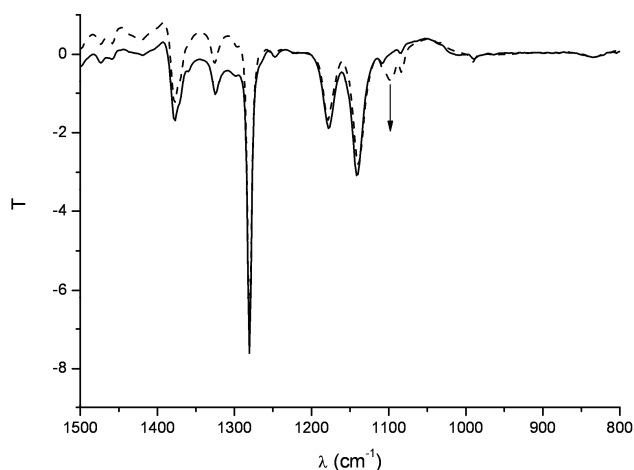


Figure 2.5 FTIR spectra of PA1 (solid line), and after addition of (*R*)-Pgl (dashed line).

Upon titration with (*R*)- or (*S*)-Pgl in a monophasic system of water-saturated dichloromethane and PA1 kept at $c = 1.0$ mM, an additional band appears at 1098 cm^{-1} . Ramirez et al²⁴ reported the appearance of bands between 1070-1080 cm^{-1} of the phosphates formed by complexation of phosphodiester and primary amines, which can be assigned to the stretching vibrations of the phosphoryl bond of the phosphate. Corresponding results were obtained by allowing equimolar amounts ($c = 10.0$ mM) of diphenyl phosphate to react in dichloromethane with *n*-octyl

amine and (*S*)-Pgl, respectively. The FTIR spectra of the resulting phosphate salts both show an absorption at 1088 cm^{-1} . These results support the formation of a phosphate in the complexation of Pgl to PA1.

These titration spectra can also be used for quantitative analysis. The results are shown in Figure 2.6. The spectra are normalized to the absorption band at 1297 cm^{-1} . In accordance with the data obtained by ^1H -NMR spectroscopy (Figure 2.4), an absorption maximum is obtained at $[\text{Pgl}]/[\text{PA1}] = 1$.

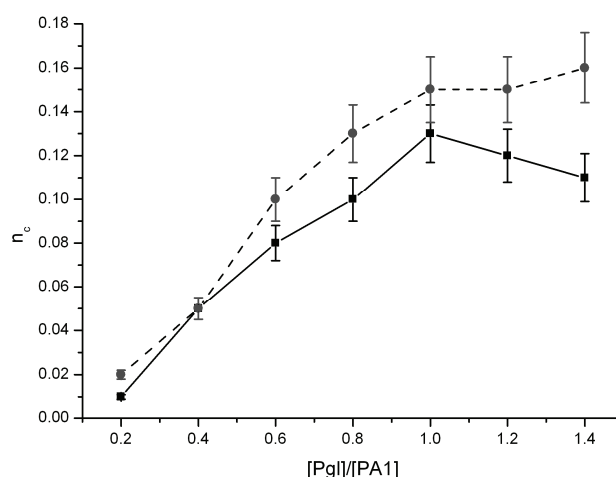


Figure 2.6 Normalized FTIR absorption values (n_c) of PA1 phosphate formation upon titration of (*R*)-Pgl (solid) and (*S*)-Pgl (dashed). Error bars represent 10 % standard deviation.

UV-Vis and CD Spectroscopy

UV-Vis and CD spectroscopy were employed to probe the effect of complexation on binding to the host in DCM as a solvent. Figure 2.7a shows the titration of Pgl in which PA1 is kept at a constant concentration ($c = 1.0\text{ mM}$). The concentration of (*R*)-Pgl was increased from 0.0 mM to 1.2 mM . Two isosbestic points can be seen at $\lambda = 307\text{ nm}$ and $\lambda = 330\text{ nm}$ in Figure 2.7. (*R*)-Pgl does not absorb at these wavelengths and the total concentration

Chapter 2

of PA1 and PA1 complexed with substrate is constant throughout the titration. The absorption reaches a maximum when (*R*)-Pgl = 1.0 mM, supporting the formation of the complex in a 1:1 ratio. A difference in absorption is observed at $\lambda = 340$ nm. Addition of the (*R*)-Pgl substrate to PA1 shows a larger increase in absorption at $\lambda = 340$ nm than seen with addition of the (*S*)-Pgl to PA1, which is most apparent in the UV-Vis differential spectra depicted in Figure 2.7b.

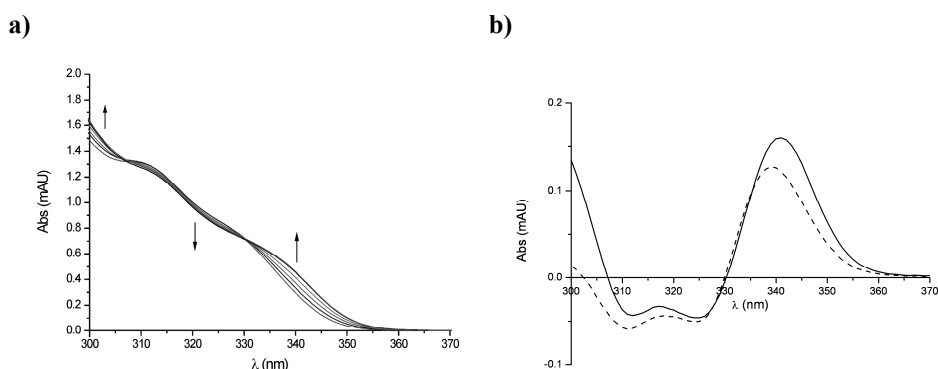


Figure 2.7 UV-Vis spectra (a) of PA1 (1.0 mM) upon titration of (*R*)-Pgl (0.0 – 1.2 mM) and differential spectra (b) of (*R*)-Pgl (1.0 mM, solid line) and (*S*)-Pgl (1.0 mM, dashed line).

A titration of PA1 with either tetra-*n*-butylammonium hydroxide (TBAOH) or triethylamine (TEA) was followed by UV-Vis and CD spectroscopy (Figure 2.8) to determine the effect of deprotonation on the spectral properties of PA1. The UV-Vis spectrum (Figure 2.8a) shows a change in absorption which is more pronounced, e.g. at $\lambda = 336$ nm, especially in the case of TBAOH, than in the case of Pgl (Figure 2.7a). A large change in molar ellipticity is observed by CD spectroscopy in this region also. Since TBAOH is a strong base, the resulting complex can be considered as a fully formed ion pair. Hence the change in ellipticity at $\lambda = 336$ nm can be attributed to deprotonation of the host. The change in electron density at the phosphate group will have an effect on the structure of the BNPA backbone

and ultimately, the observed ellipticity, due to the C_2 symmetry in the BNPA backbone, changes.²⁵

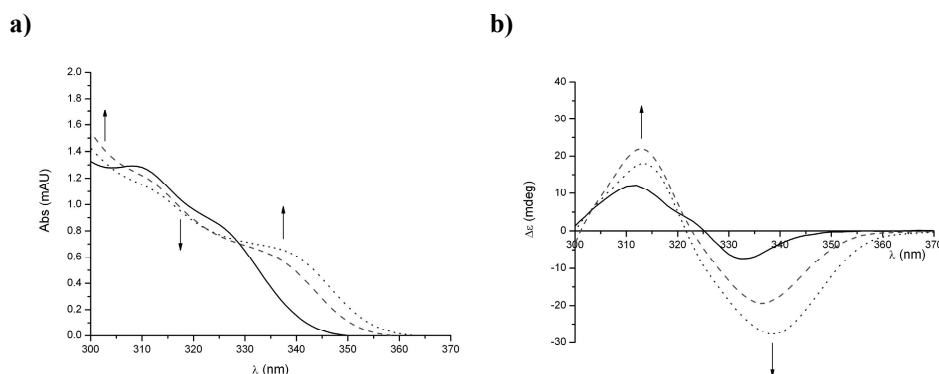


Figure 2.8 UV-Vis (a) and CD spectra (b) of PA1 (1.0 mM) before and after addition of TEA (5.0 mM, dashed) or TBAOH (5.0 mM, dotted).

Examination of the change in absorption and ellipticity at both $\lambda = 312$ and $\lambda = 336$ nm shows that the changes are different for the PA1-TEA complex compared to the PA1-TBAOH complex. Both the change in absorption in the UV-Vis spectrum at $\lambda = 336$ nm (Figure 2.8a) and the change in ellipticity at $\lambda = 336$ nm in the CD spectrum (Figure 2.8b) are less pronounced in the case of PA1-TEA compared to PA1-TBAOH. This is possibly due to the PA1-TEA complex having more hydrogen-bonding character or forming a tighter ion pair. In contrast, the change in ellipticity at $\lambda = 312$ nm is more pronounced for PA1-TEA than PA1-TBAOH. This may be due to a change in conformation of PA1, caused by steric interactions with TEA, i.e. a tighter ion pair with PA1 than observed with TBAOH.

The CD spectra obtained while following the titration of (*R*)-Pgl and (*S*)-Pgl to PA1 are shown in Figure 2.9. The CD spectra show an increase in ellipticity both at $\lambda = 314$ nm and $\lambda = 336$ nm. The change in magnitude of the ellipticity at $\lambda = 336$ nm is relatively less pronounced than in those cases

Chapter 2

using TEA and TBAOH (Figure 2.8b). This is an indication that the binding of the Pgl substrates to PA1 has a strong hydrogen-bonding character, more than it resembles the formation of a fully dissociated ion pair. The binding of both enantiomers of Pgl to PA1 results in a corresponding change in ellipticity at $\lambda = 336$ nm.

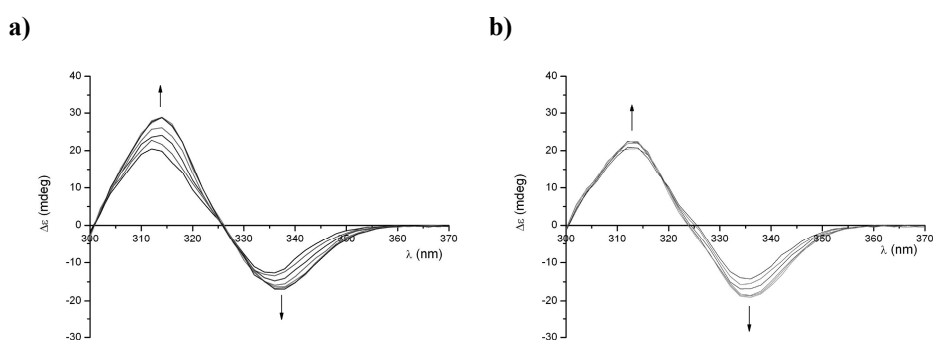


Figure 2.9 CD spectra of PA1 (1.0 mM) upon titration of (*R*)-Pgl (a) and (*S*)-Pgl (b) (0.0 – 1.2 mM)

The change in ellipticity at $\lambda = 314$ nm is more pronounced for (*R*)-Pgl (Figure 2.9a) than for (*S*)-Pgl (Figure 2.9b). The higher ellipticity of (*R*)-Pgl at $\lambda = 314$ nm compared to (*S*)-Pgl can be ascribed to a change of the conformation of PA1, which may be a result of steric interactions upon the formation of the PA1-(*R*)-Pgl complex, comparable to the change of ellipticity observed for the PA1-TEA complex (Figure 2.8b). It should be noted that the single extraction experiments *vide supra* showed that (*S*)-Pgl is the preferred enantiomer in extraction. The additional steric interactions indicated by CD spectroscopy for (*R*)-Pgl may be related to the preference for (*S*)-Pgl, i.e. (*S*)-Pgl requires less disturbance to the PA1 backbone and hence the Gibbs energy of complexation is lower.

2.2.3 Transport experiments and reversibility

Reversibility of the complexation of Pgl to PA1 was demonstrated by bulk-membrane transport experiments. The U-tube depicted in Figure 2.10 was used to transport Pgl from the feeding phase to the receiving phase via the transport phase, using PA1 as an enantioselective carrier.

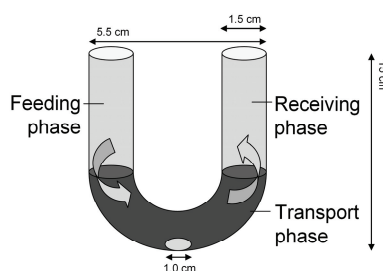


Figure 2.10 Bulk membrane transport system

Table 2.6 Bulk membrane transport numbers.

t (h)	$[Pgl]$ (aq) (receiving phase)	ee (aq) (receiving phase)
2.0	0.07	24
3.0	0.10	24
4.0	0.21	23
5.0	0.27	23
6.0	0.38	23
22.0	3.46	16

Conditions: feeding phase: $V_{fp} = 5.0$ mL; aqueous phosphate buffer (0.100 M) pH = 5.0; $c(Pgl) = 20$ mM. Transport phase: $V_{tp} = 10.0$ mL; carbon tetrachloride; $c(PA1) = 0.5$ mM. Receiving phase: $V_{rp} = 5.0$ mL; aqueous phosphate buffer (0.100 M); pH = 2.2.

The bulk membrane transport experiment shows that the host PA1 is able to transport the substrate PGL catalytically through the bulk membrane (Table 2.6). The ee of the receiving phase decreases with time as a result of the change in concentrations in the feeding phase. The transport experiments demonstrate the reversible nature of the host-substrate complexation, which can be controlled by the pH of the aqueous phases.

2.3 Conclusions and outlook

We have shown that chiral BINOL-based phosphoric acids can be used in the enantioselective liquid-liquid extraction of amines and amino alcohols. Both the nature of the host as well as the substrate are important in optimizing the operational selectivity. The distribution can be controlled by the pH of the buffered aqueous phase. In the case of Mba extracted by PA1, the operational selectivity shows a dependency on the polarity of the organic phase: the lower the polarity, the higher the selectivity. This may be either due to ion pair formation or the decreased amount of water in the organic phase. The ee in both phases can be controlled by tuning both the pH and the stoichiometry of the host with respect to the substrate. However, this has no effect on the operational selectivity. Bulk membrane transport experiments demonstrate the possibility of catalytic enantioselective transport and reversible extraction.

Titration studies followed by ^1H -NMR and FTIR spectroscopy confirm the formation of a 1:1 complex of the phosphoric acid host and the primary amine substrate. Formation of a 1:1 complex is also demonstrated by UV-Vis and CD spectroscopy. The CD spectra suggest a relation between the change in magnitude of the ellipticity and the mechanism of complexation of the substrate to the host. Additional interaction of the unfavored substrate is presumed to be responsible for the enantioselectivity of the host with respect to the substrate. The bulk membrane transport experiments establish the reversibility of the system. For the application in a cascade (which is covered in Chapter 3), the system meets the required properties such as a sufficient selectivity for a number of substrates, full reversibility and control of distribution.

2.4 Experimental section

2.4.1 Instrumentation

NMR spectra were recorded on a Varian Mercury Plus 200 (^1H NMR at 200 MHz, ^{13}C NMR at 50 MHz) or on a Varian Mercury Plus 400 (^1H NMR at 400 MHz, ^{13}C NMR at 100 MHz). Chemical shifts (δ) are denoted in ppm and referenced to the residual solvent peak unless stated otherwise (CDCl_3 , ^1H δ = 7.24, ^{13}C δ = 77.0).²⁶ The splitting patterns are designated as follows: s (singlet), d (doublet), dd (double doublet), t (triplet), q (quartet), m (multiplet) and br (broad). Coupling constants (J) are denoted in Hertz (Hz).

Electron impact (MS-EI+), and exact mass determination (HRMS) were recorded on a AEI MS-902 instrument. Elemental analysis was performed on a EuroVector CHNS-O Elemental Analyzer Euro EA 3000. Melting points were recorded on a Büchi B-545 melting point apparatus. UV-Vis spectra were recorded on a Jasco V-630 Spectrophotometer. FTIR spectra were recorded on a Nicolet Nexus FT-IR. CD spectra were recorded on a Jasco J-715 Spectropolarimeter. The pH of the aqueous solutions was measured using a Hanna Instruments pH 213 Microprocessor pH meter.

2.4.2 Extraction experiments and chemical analysis

All extraction experiments were carried out in 1.5 mL screw capped vials. In a standard experiment, a 1.0 mM solution of the host in the organic phase was combined with a 2.0 mM solution of the substrate in the buffered aqueous solution in equivolumous amounts (0.40 mL). Reactions were carried out *in duplo* and with a simultaneous blank extraction ($c(\text{host}) = 0.0$ mM) to determine the physical partition of the substrate. The two phase systems were stirred overnight at $T = 6\text{ }^\circ\text{C}$ and subsequently allowed to settle for at least 30 min. The aqueous phase was analyzed by RP-HPLC, using Shimadzu CC-20AD pumps, a Crownpak CR(+) chiral column (Daicel, Japan) equipped with a guard column and a SPD-M20A diode array

Chapter 2

detector. A calibration curve was prepared in the concentration range employed for the determination of the distribution. Uncertainties were typically between 0.5-2.0 %. Perchloric acid solutions (pH = 1.0, 1.5 or 2.0) were used as eluent for the RP-HPLC analysis.

2.4.3 U-tube experiments

Feeding phase: $V_{fp} = 5.0$ mL; aqueous phosphate buffer (0.100 M) pH = 5.0; $c(\text{Pgl}) = 20$ mM. Transport phase: $V_{tp} = 10.0$ mL; carbon tetrachloride; $c(\text{PA1}) = 0.5$ mM. Receiving phase: $V_{rp} = 5.0$ mL; aqueous phosphate buffer (0.100 M); pH = 2.2. The phases were placed into the U-tube according to Figure 2.10. The tube was placed in a cooled chamber at $T = 6$ °C. The magnetic stirrer was set to 900 rpm. For analysis, aliquots of 0.20 mL were removed from the receiving phase and were replaced by 0.2 mL of buffer.

2.4.4 Titration experiments followed by spectroscopy

Organic solvents were pre-saturated with water and were employed to make stock solutions of the host and the substrate. The stock solutions were mixed in a vial and shaken vigorously before the measurements. Dcm was used for the UV-Vis, CD and FTIR experiments. Deuterated chloroform was used as the organic solvent for the NMR experiments. Single extraction experiments with deuterated chloroform gave results corresponding to extractions with normal chloroform.

2.4.5 Chemicals and methods

(*R*)- and (*S*)-2-Phenylglycinol (98%), *rac*-2-phenylglycinol (98%), *rac*-norephedrine hydrochloride (99+%), (*R*)- and (*S*)- α -methylbenzylamine (99%), *rac*- α -methylbenzylamine (99%) were obtained from Acros. *rac*-1-Aminoindan (98%), (*R*)- and (*S*)-aminoindan, (*1R,2R*)-(-)-*trans*-1-amino-2-indanol (97%), (*1S,2S*)-(-)-*trans*-1-amino-2-indanol (97%), (*1S,2R*)-(-)-*cis*-1-amino-2-indanol (97%), (*1R,2S*)-(-)-*cis*-1-amino-2-indanol (97%) were obtained from Sigma-Aldrich. (*S*)-1-Phenylpropylamine (99%) and (*R*)-1-

Chiral Separation of Primary Amines with Phosphoric Acids

phenylpropylamine (99%) were obtained from Alfa Aesar. Water was doubly distilled prior to use.

All buffers were prepared using NaH_2PO_4 , obtained from Merck at a concentration of 100 mM and subsequent addition of HCl (aq) or NaOH (aq).

The phosphoric acids used in the study were prepared according to the reaction scheme depicted in Figure 2.11.

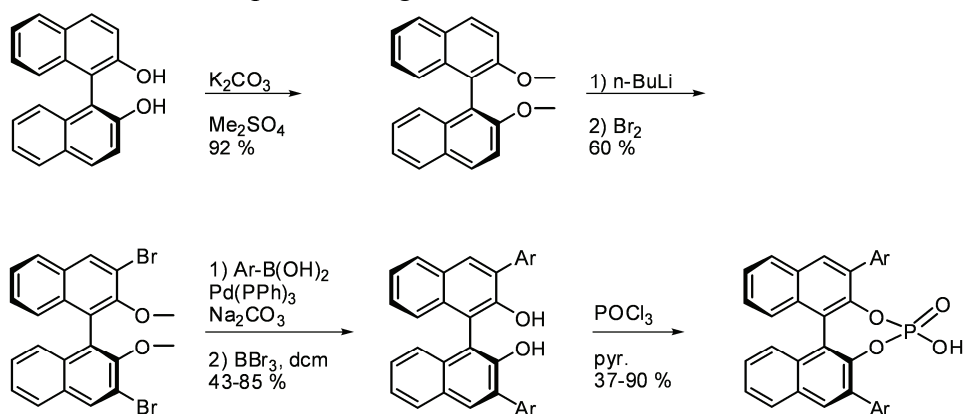
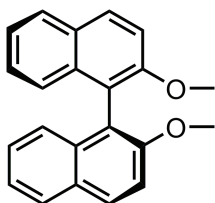


Figure 2.11 General reaction scheme (Ar = aromatic group).

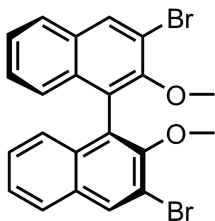
Chapter 2

Preparation of (S)-2,2'-dimethoxy-1,1'-binaphthyl.



(S)-BINOL (50 g, 0.18 mol) was dissolved in acetone (1 L). K_2CO_3 (823 g, 0.6 mol) was added and the suspension was stirred for 15 min. Me_2SO_4 (50 g, 67.6 mL, 0.40 mol) was added dropwise. The reaction mixture was stirred overnight and filtered. The solvent was evaporated *in vacuo*, giving (S)-2,2'-dimethoxy-1,1'-binaphthyl (52 g, 92 %) as a white powder. $[\alpha]_D^{20} = -564.0$ (c 1.00, $CHCl_3$). M.p. 195-199 °C. 1H NMR (400 MHz, $CDCl_3$) δ ppm 7.96 (d, $J = 9.00$ Hz, 2H), 7.85 (d, $J = 8.12$ Hz, 2H), 7.45 (d, $J = 9.03$ Hz, 2H), 7.30 (m, 2H), 7.19 (m, 2H), 7.09 (dd, $J = 8.52, 0.59$ Hz, 2H), 3.75 (s, 6H). ^{13}C NMR (50 MHz, $CDCl_3$): δ ppm 155.2, 134.2, 129.6, 129.4, 128.1, 126.5, 125.5, 123.7, 119.8, 114.5, 57.1; MS(EI+): 314 $[M^+]$.

Preparation of (S)-3,3'-dibromo-2,2'-dimethoxy-1,1'-binaphthyl.

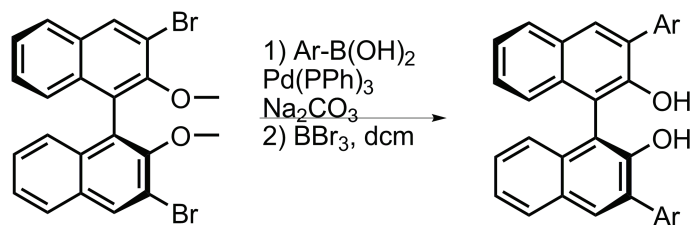


(S)-2,2'-Dimethoxy-1,1'-binaphthyl (25.0 g, 79.5 mmol) was suspended in Et_2O dried over sodium (0.7 L) and the mixture was mechanically stirred under a nitrogen atmosphere at rt. TMEDA (38 mL), dried over Na_2SO_4 , was added followed by dropwise addition of n-BuLi (2.5 M in hexanes, 140 mL, 0.35 mol, 4.4 eq.). The reaction mixture was stirred overnight and turned from a white suspension into a light brown suspension. A conversion check by quenching a sample with Br_2 showed full conversion. The reaction mixture was cooled to -80 °C and Br_2 (35 mL, 0.69 mol) was added

Chiral Separation of Primary Amines with Phosphoric Acids

dropwise over a period of 1h. The reaction mixture was stirred for one more hour at -80 °C and allowed to warm to -10 °C. A saturated aqueous solution of Na₂SO₃ (400 mL) was added dropwise and the reaction mixture was stirred overnight at rt. The layers were separated and the aqueous phase was subsequently extracted with EtOAc and DCM. The combined organic layers were dried with brine and Na₂SO₄ and the solvent was removed *in vacuo*. The crude product was filtered over silica (eluent: EtOAc:pentane 1:1) and triturated in ether. The obtained solid was dried for 16h in a vacuum oven at T = 40 °C giving (*S*)-3,3'-dibromo-2,2'-dimethoxy-1,1'-binaphthyl (22.6 g, 60 %) as an off-white powder. $[\alpha]_D^{20} = -121.0$ (c 1.00, CHCl₃). M.p. 157-159 °C. ¹H NMR (400 MHz, CDCl₃) δ ppm 8.27 (s, 2H), 7.82 (d, *J* = 8.15 Hz, 2H), 7.42 (m, 2H), 7.27 (m, 2H), 7.08 (d, *J* = 8.50 Hz, 2H), 3.51 (s, 6H),). ¹³C NMR (50 MHz, CDCl₃): δ ppm 133.3, 133.2, 131.7, 127.3, 127.1, 126.1, 126.0, 117.7, 61.3; MS(EI+): 472 [M⁺].

General procedure for the preparation of (*S*)-3,3'-diaryl-2,2'-dimethoxy-1,1'-binaphthyls.

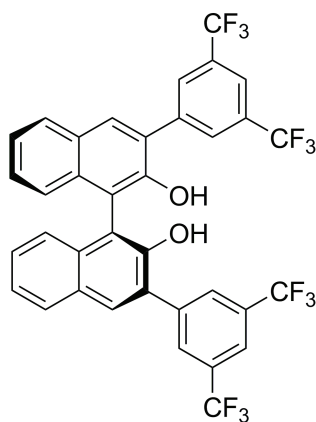


A literature procedure of Chong *et al.*²⁷ was followed for the Suzuki coupling used for this synthesis. (*S*)-3,3'-Dibromo-2,2'-dimethoxy-1,1'-binaphthyl (typically 500 mg) and Pd(PPh₃)₄ (0.1 eq.) were dissolved in DME (2.5 mL). The reaction mixture was flushed three times with Ar. The aryl boronic acid (3.5 eq.) was added, followed by an aqueous 2 M Na₂CO₃ (0.56 mL) solution. The reaction mixture was flushed three more times with Ar and stirred for 16h at 95 °C. TLC revealed full conversion. The reaction mixture was filtered over Celite and the solvent of the filtrate was evaporated *in vacuo*. The crude product was dissolved in DCM, washed with sat. NH₄Cl (aq), water and brine and dried over Na₂SO₄. The solvent

Chapter 2

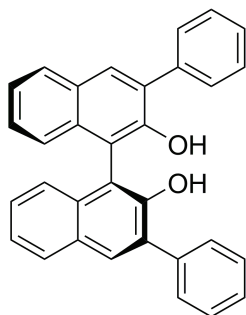
was evaporated *in vacuo*. The crude product was dissolved in DCM (100 mL) and the solution was cooled in an ice-bath. A solution of BBr₃ (10 eq.) in DCM (10 mL) was added dropwise. The reaction mixture was allowed to warm to room temperature and stirred for 16h. ¹H-NMR analysis revealed complete conversion. The resulting mixture was cooled in an ice bath and ice water was added dropwise. The reaction mixture was stirred for 1h and sat. aqueous NaHCO₃ solution was added dropwise. The layers were separated, the organic layer was washed with water and brine and dried over Na₂SO₄. The solvent was evaporated *in vacuo*. The crude product was purified using silica gel chromatography (eluent: pentane, 5 v-% EtOAc) yielding the (*S*)-3,3'-diaryl-2,2'-hydroxy-1,1'-binaphthyl.

(*S*)-3,3'-Bis(3,5-ditrifluoromethyl)phenyl)-2,2'-dihydroxy-1,1'-binaphthyl.



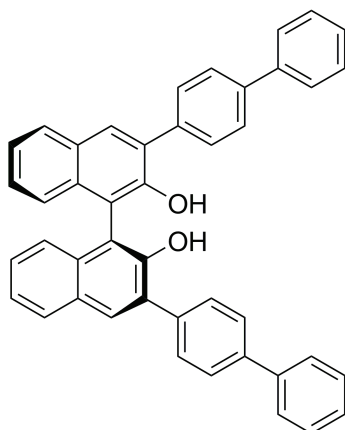
The product was obtained as a white powder (23.4 g, 85 %). $[\alpha]_D^{20} = -35.4$ (c 1.00, CHCl₃). M.p. 97-99 °C. ¹H NMR (400 MHz, CHCl₃): δ 8.24-8.20 (m, 4H), 8.12-8.09 (m, 2H), 7.99 (d, *J* = 7.75 Hz, 2H), 7.92-7.89 (m, 2H), 7.47 (m, 2H), 7.41 (m, 2H), 7.22 (d, *J* = 7.94 Hz, 2H), 5.35 (d, *J* = 0.52 Hz, 2H). ¹³C NMR (50 MHz, CDCl₃): δ 144.1, 144.0, 139.0, 132.6, 132.1, 131.9, 131.5, 131.3, 130.2, 128.8, 127.68, 127.3, 126.8, 126.1, 122.9, 120.7. MS(EI⁺): 710 [M⁺]. Anal. Calcd for C₃₆H₁₈F₁₂O₂: C, 60.86; H, 2.55; Found: C, 60.74 H, 2.57.

(S)-3,3'-Bis-2-phenyl-2,2'- dihydroxy -1,1'-binaphthyl.



The product was obtained as a white powder (0.20 g, 45 %). $[\alpha]_D^{20} = -71.8$ (c 1.00, CHCl_3); M.p. 203-205 °C; ^1H NMR (400 MHz, CDCl_3): δ 8.03 (d, $J = 0.60$ Hz, 2H), 7.93 (d, $J = 8.09$ Hz, 2H), 7.74 (dd, $J = 7.22, 1.10$ Hz, 4H), 7.50 (m, 4H), 7.41 (m, 4H), 7.32 (m, 2H), 7.29-7.21 (m, 2H), 5.47-5.26 (s, 2H). ^{13}C NMR (50 MHz, CDCl_3): δ 112.6, 124.5, 124.6, 127.6, 128.0, 128.7, 128.8, 129.7, 129.8, 130.9, 131.6, 133.2, 137.7, 150.4. MS: 438.2 $[\text{M}^+]$; Anal. Calcd for $\text{C}_{32}\text{H}_{22}\text{O}_2$: C, 87.65; H, 5.06 Found: C, 87.18 H, 5.14.

(S)-3,3'-Bis-2-(4-phenyl)-phenyl-2,2'- dihydroxy -1,1'-binaphthyl.

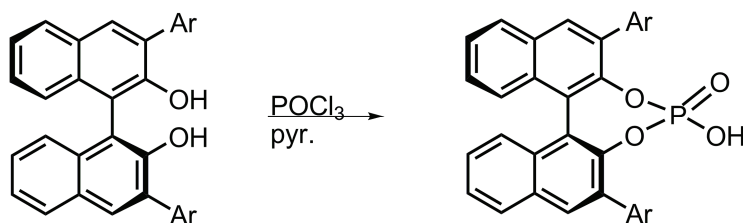


The product was obtained as a white powder (1.38 g, 43 %). $[\alpha]_D^{20} = +65.4$ (c 1.00, CHCl_3). M.p. 219-222 °C. ^1H NMR (400 MHz, CDCl_3): δ 8.12-8.09 (s, 2H), 7.96 (d, $J = 7.95$ Hz, 2H), 7.85 (d, $J = 8.08$ Hz, 4H), 7.74 (d, $J =$

Chapter 2

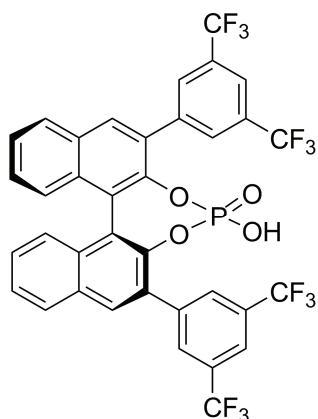
8.11 Hz, 4H), 7.68 (d, $J = 8.23$ Hz, 4H), 7.48 (t, $J = 7.64$ Hz, 4H), 7.45-7.32 (m, 2H), 7.29-7.24 (m, 6H), 5.44-5.41 (s, 2H). ^{13}C NMR (50 MHz, CDCl_3): δ ppm 112.6, 124.5, 124.7, 127.4, 127.5, 127.7, 128.8, 129.1, 129.8, 130.3, 130.5, 131.7, 133.2, 136.7, 140.9, 141.0, 150.5. MS: 590 [M^+]; Anal. Calcd for $\text{C}_{44}\text{H}_{30}\text{O}_2$: C, 89.46; H, 5.12; Found: C, 89.38; H, 5.12.

General procedure for the preparation of (S)-3,3'-Diaryl-2,2'-diyl hydrogenphosphate-1,1'-binaphthyls.



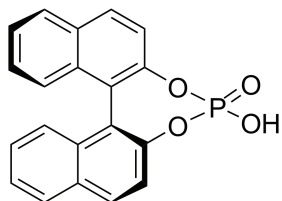
A modified literature procedure of Akiyama *et al.*²³ was followed for the phosphoric acid synthesis. The (S)-3,3'-diaryl-2,2'-hydroxy-1,1'-binaphthyl (typically 50 mg) was dissolved in pyridine (1 mL) and POCl_3 (2.0 eq.) was added at rt. The reaction mixture was stirred overnight. TLC revealed full conversion. The reaction mixture was cooled in an ice-bath and water (1 mL) was added carefully. The reaction mixture was stirred for 30 min at rt. and DCM (30 mL) was added. Subsequently, 1 M HCl (aq., 30 mL) was added and the layers were separated. The solvent of the organic phase was evaporated *in vacuo* and the product was purified using C18RP-silica chromatography using a water/MeOH gradient. The fractions containing pure product were collected and the solvent was evaporated *in vacuo*. The product was stripped with toluene and dried 16 h in a vacuum oven at 40 °C.

(S)-3,3'-bis(3,5-Ditrifluoromethyl)phenyl)-2,2'-diyl hydrogenphosphate-1,1'-binaphthyl (PA1).



The product was obtained as a white powder²³ (1.2 g, 37 %). $[\alpha]_D^{20} = +238$ (c 1.00, CHCl₃). M.p. 174-180 °C (dec). ¹H NMR (400 MHz, CDCl₃): δ 8.91 (s, 1H), 8.12 – 7.85 (m, 8H), 7.57 (m, 4H), 7.45 – 7.29 (m, 4H). ¹³C NMR (50 MHz, CDCl₃): δ 143.5, 138.6, 132.3, 132.0, 131.4, 131.4, 131.1, 129.9, 128.7, 127.6, 127.1, 126.8, 123.1, 122.5, 121.5. ³¹P NMR (189 MHz, CDCl₃): δ 6.0 ppm (s). ¹⁹F NMR (376 MHz, CDCl₃): δ -62.6 (s). HRMS (EI⁺) calcd for C₃₆H₁₈F₁₂O₄P: m/z 773.0751; found 773.0750. IR(DCM) 3522, 1622, 1597, 1502, 1474, 1462, 1427, 1377, 1358, 1335, 1281, 1236, 1182, 1140, 1036, 989 cm⁻¹.

(S)-2,2'-Diyl hydrogen phosphate-1,1'-binaphthyl (PA2).

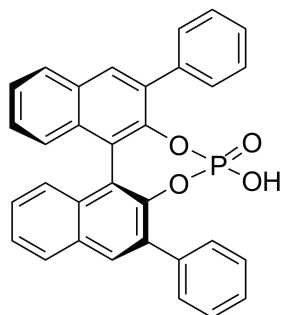


The product was obtained as a white powder²³ (0.40 g, 90 %). $[\alpha]_D^{20} = +457$ (c 1.00, CHCl₃). M.p. 232-235 °C (dec). ¹H NMR (200 MHz, CDCl₃): δ 8.69 (d, $J = 5.45$ Hz, 1H), 8.04 (t, $J = 8.13$ Hz, 1H), 7.87 (d, $J = 8.47$ Hz, 4H), 7.55 (d, $J = 8.84$ Hz, 2H), 7.41 (dd, $J = 13.43, 7.14$ Hz, 4H), 7.32-7.20

Chapter 2

(m, 1H); ^{13}C NMR (50 MHz, CDCl_3): δ 142.4, 132.6, 131.6, 130.9, 128.6, 127.3, 126.5, 125.4, 122.1, 121.6; MS(EI+): 348 $[\text{M}^+]$, HRMS (EI+) calcd for $\text{C}_{20}\text{H}_{14}\text{O}_4\text{P}$: m/z 349.0630; found 349.0624.

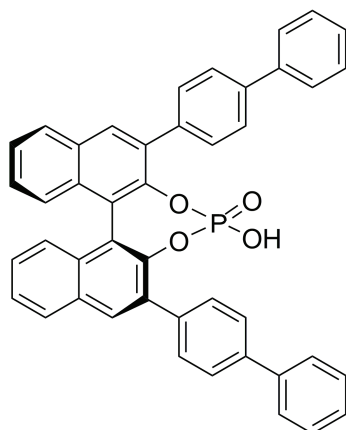
(S)-3,3'-Diphenyl-2,2'-diyl hydrogen phosphate-1,1'-binaphthyl (PA3).



The product was obtained as a white powder²⁸ (0.12 g, 48 %). $[\alpha]_{\text{D}}^{20} = +337$ (c 1.00, CHCl_3). M.p. 194-197 °C (dec). ^1H NMR (400 MHz, CDCl_3): δ 8.56 – 8.32 (m, 1H), 7.99 (s, 2H), 7.95 (d, $J = 8.2$ Hz, 2H), 7.58 (d, $J = 7.2$ Hz, 4H), 7.53 – 7.45 (m, 2H), 7.38 (d, $J = 8.3$ Hz, 2H), 7.34 – 7.27 (m, 2H), 7.27 – 7.20 (m, 4H), 7.17 (d, $J = 7.3$ Hz, 2H). ^{13}C NMR (50 MHz, CDCl_3): δ 144.9, 144.7, 137.0, 134.3, 132.2, 131.8, 131.5, 128.6, 128.4, 127.8, 127.3, 126.7, 126.2, 122.6 ppm. ^{31}P NMR (189 MHz, CDCl_3): δ 4.2 ppm (s). MS: 500 $[\text{M}^+]$, HRMS (EI+) calcd for $\text{C}_{21}\text{H}_{14}\text{O}_4\text{PNa}$: m/z 523.1075 found: 523.1048.

Chiral Separation of Primary Amines with Phosphoric Acids

(S)-3,3'-Bis-2-(4-Phenyl)-phenyl-2,2'-diyl hydrogen phosphate-1,1'-binaphthyl (PA4).



The product was obtained as a white powder (0.13 g, 59 %). $[\alpha]_D^{20} = +357$ (c 1.00, CHCl_3). M.p. 220-223 °C (dec). ^1H NMR (400 MHz, CDCl_3): δ 8.02 (s, 2H), 7.96 (d, $J = 8.1$ Hz, 2H), 7.61 (d, $J = 8.1$ Hz, 4H), 7.51 (t, $J = 7.0$ Hz, 2H), 7.46 – 7.28 (m, 12H), 7.17 (d, $J = 3.6$ Hz, 6H). ^{13}C NMR (50 MHz, CDCl_3): δ 144.8, 144.6, 141.0, 140.7, 135.8, 133.9, 133.8, 132.1, 131.8, 131.6, 130.3, 128.7, 127.4, 127.2, 126.8, 126.7, 126.3, 122.6. ^{31}P NMR (162 MHz, CDCl_3): δ ppm 5.02 (s). MS: 652 $[\text{M}^+]$; HRMS (EI^+) calcd for $\text{C}_{44}\text{H}_{30}\text{O}_4\text{PNa}$: m/z 653.1882 found: 653.1876.

2.5 References and notes

1. Peacock, S. C.; Domeier, L. A.; Gaeta, F. C. A.; Helgeson, R. C.; Timko, J. M.; Cram, D. J. *J. Am. Chem. Soc.* **1978**, *100* (26), 8190-8202.
2. Lingenfelter, D. S.; Helgeson, R. C.; Cram, D. J. *J. Org. Chem.* **1981**, *46* (2), 393-406.
3. Yamamoto, K.; Isoue, K.; Sakata, Y.; Kaneda, T. *J. Chem. Soc. Chem. Comm.* **1992**, (10), 791-793.
4. Steensma, M. *Chiral Separation of amino-alcohols and amines by fractional reactive extraction*; 2005.
5. Tang, L.; Choi, S.; Nandhakumar, R.; Park, H.; Chung, H.; Chin, J.; Kim, K. M. *J. Org. Chem.* **2008**, *73* (15), 5996-5999.
6. Steensma, M.; Kuipers, N. J. M.; De Haan, A. B.; Kwant, G. *Chirality* **2006**, *18* (5), 314-328.
7. Van de Voorde, I.; Pinoy, L.; Courtijn, E.; Verpoort, F. *Solvent Extr. Ion Exch.* **2006**, *24* (6), 893-914.
8. Teramoto, M.; Yamashiro, T.; Inoue, A.; Yamamoto, A.; Matsuyama, H.; Miyake, Y. *J. Membr. Sci.* **1991**, *58* (1), 11-32.
9. Tan, B.; Luo, G. S.; Wang, H. D. *Tetrahedron Asym.* **2006**, *17* (6), 883-891.
10. Akiyama, T. *Chem. Rev.* **2007**, *107* (12), 5744-5758.
11. Martinborough, E.; Denti, T. M.; Castro, P. P.; Wyman, T. B.; Knobler, C. B.; Diederich, F. *Helv. Chim. Acta* **1995**, *78* (5), 1037-1066.
12. Tamada, J. A.; King, C. J. *Ind. Eng. Chem. Res.* **1990**, *29* (7), 1327-1333.
13. King, C. J. *Chemtech* **1992**, *22* (5), 285-291.
14. Schug, K. A.; Lindner, W. *Chem. Rev.* **2005**, *105* (1), 67-113.
15. Anslyn, E. V.; Dougherty, D. A. *Modern Physical Organic Chemistry*; University Science Books: Sausalito, Calif., 2006.
16. Kellner, K. H.; Blasch, A.; Chmiel, H.; Lammerhofer, M.; Lindner, W. *Chirality* **1997**, *9* (3), 268-273.
17. Wanner, M. J.; van der Haas, R. N. S.; de Cuba, K. R.; van Maarseveen, J. H.; Hiemstra, H. *Angew. Chem. Int. Ed.* **2007**, *46* (39), 7485-7487.
18. Liljefors, T.; Norrby, P. O. *J. Am. Chem. Soc.* **1997**, *119* (5), 1052-1058.
19. Quin, L. D. In *A Guide to Organophosphorus Chemistry*, John Wiley & Sons, Ed.; New York, 2000; p 133.
20. Schuur, B. Enantioselective liquid-liquid extraction in centrifugal contactor separators. 2008.
21. Lehn, J. M. *Supramolecular chemistry : concepts and perspectives*; Weinheim : VCH: 1995.
22. Dykes, G. M.; Smith, D. K.; Caragheorgheopol, A. *Org. Biomol. Chem.* **2004**, *2* (6), 922-926.
23. Akiyama, T.; Morita, H.; Itoh, J.; Fuchibe, K. *Org. Lett.* **2005**, *7* (13), 2583-2585.
24. Ramirez, F.; Marecek, J. F.; Ugi, I. *J. Am. Chem. Soc.* **1975**, *97* (13), 3809-3817.
25. Kato, N. *J. Am. Chem. Soc.* **1990**, *112* (1), 254-257.
26. Gottlieb, H. E.; Kotlyar, V.; Nudelman, A. *J. Org. Chem.* **1997**, *62* (21), 7512-7515.

Chiral Separation of Primary Amines with Phosphoric Acids

27. Wu, T. R.; Shen, L. X.; Chong, J. M. *Org. Lett.* **2004**, 6 (16), 2701-2704.
28. Yamanaka, M.; Itoh, J.; Fuchibe, K.; Akiyama, T. *J. Am. Chem. Soc.* **2007**, 129 (21), 6756-6764.

Chapter 2